Infrared Cyclotron Resonance in InSb

E. D. Palik, G. S. Picus,* S. Teitler, and R. F. Wallis

U. S. Naval Research Laboratory, Washington, D. C.

(Received November 14, 1960; revised manuscript received January 23, 1961)

Far-infrared cyclotron resonance absorption in n-type InSb has been measured to determine the variation of the conduction electron effective mass with magnetic field. At high magnetic fields the absorption was resolved into a strong line with a weaker satellite line at lower photon energy and a broad, weak absorption at still lower energy. The interpretation of this structure in terms of the conduction-band properties of InSb is discussed.

1. INTRODUCTION

MICROWAVE cyclotron resonance absorption in InSb was observed by Dresselhaus et al.,[1] who determined the conduction-electron effective mass and a heavy-hole effective mass. Burstein, Picus, and Gebbie[2] measured infrared cyclotron absorption and reflection in InSb and demonstrated that in the infrared the $\omega_c\tau > 1$ requirement is easier to meet than in the microwave region. Pulsed-magnetic-field cyclotron absorption and reflection measurements were performed by Keyes et al.,[3] who showed that the conduction-electron effective mass increases with increasing magnetic field, an indication of the nonparabolic nature of the conduction band. Also, Lipson, Zwerdling, and Lax[4] measured cyclotron resonance reflection in the far infrared. A review of work to date on cyclotron resonance has been given by Lax and Mavroides.[5]

We have measured cyclotron resonance absorption in the far infrared from 63 cm^{-1} (155 μ) to 340 cm^{-1} (29 μ) to determine the variation of effective mass with magnetic field. At high fields, a strong absorption line was observed along with a weaker satellite line to lower energy, and a broad, weak absorption to still lower energy. This additional structure is probably due to transitions between various, nonequally spaced Landau levels and is discussed in detail in Sec. 4.

2. EXPERIMENTAL TECHNIQUES

The NRL Bitter solenoidal magnet has been used to obtain steady fields as high as 70 kilogauss. The measurements have been made at three temperatures, 300°K, 80°K, and 25°K. For the room-temperature measurements the sample was simply taped to a suitable frame and inserted into the magnet. For the low-temperature measurements the sample, mounted on silicon, was attached to the cold copper block of the

Dewar with GE 7031 cement. The effect of sample strain on the present data is not known. The sample could be mounted, so that the Poynting vector **S** of the radiation field was either parallel or perpendicular to the magnetic field **H**. Sample orientation in the beam is shown in Fig. 1. The sample plane was the (100) plane. The Dewar was equipped with polyethylene, crystal quartz, or CsBr windows depending on the wavelength region being surveyed. The sample, an n-type piece of InSb with $n \approx 10^{15}$/cm^3 and $\mu = 267\,000$ cm^2/volt sec at 80°K, was glued to the silicon backing with cellulose caprate thermoplastic cement and ground and polished to a thickness of about 15 microns.

Two basic optical systems were used, one employing a prism or grating monochromator and one employing a reststrahlen monochromator. These are shown sche-
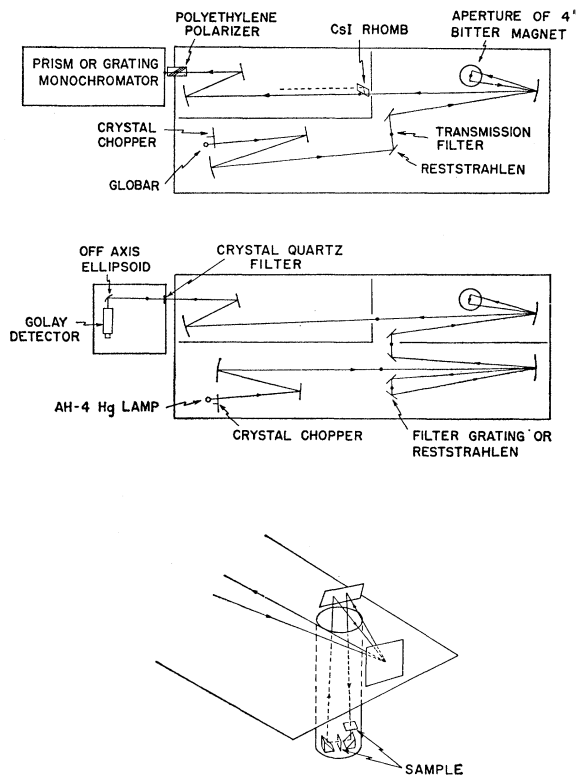
* Now at Hughes Semiconductors Products Division, Newport Beach, California.

[1] G. Dresselhaus, A. F. Kip, C. Kittel, and G. Wagoner, Phys. Rev. 98, 556 (1955).

[2] E. Burstein, G. S. Picus, and H. A. Gebbie, Phys. Rev. 103, 825 (1956).

[3] R. J. Keyes, S. Zwerdling, S. Foner, H. H. Kolm, and B. Lax, Phys. Rev. 104, 1804 (1956).

[4] H. Lipson, S. Zwerdling, and B. Lax, Bull. Am. Phys. Soc. 3, 218 (1958).

[5] B. Lax and J. G. Mavroides, in *Solid-State Physics*, edited by F. Seitz and D. Turnbull, (Academic Press, Inc., New York, 1960), Vol. 11.

FIG. 1. Optical arrangements for infrared cyclotron resonance absorption measurements.

matically in Fig. 1. For the lower frequency infrared region where energy is scarce, the reststrahlen monochromator was used to provide a broad band of energy, whereas at the higher frequency where energy is more plentiful, a CsI prism or grating monochromator providing improved resolution was used. To reduce the effects of water vapor absorption, the entire optical path was covered with a vinyl plastic tent and the air dried with a molecular sieve.

Two types of measurements were made, fixing the wavelength and varying the magnetic field, and fixing the magnetic field and varying the wavelength. In the high-frequency region, where there is sufficient energy, circularly polarized light was used to determine the sign of the charge carrier. The proper polarization was obtained using a CsI Fresnel rhomb in conjunction with a ten-sheet pile-of-plates polyethylene polarizer. The orientation of the sample was such that $S\|H$.

The principal uncertainty in the measurements is the average wavelength of the energy passed by the optical system when using the reststrahlen monochromator. Two or three crystal reflections were employed to isolate a narrow band of wavelengths. The average wavelength of this radiation was obtained by correcting the energy distribution of the source, assumed to be a blackbody, by the reflectivity of three reststrahlen plates, and the transmission of the crystal quartz filter. The results indicated that this average wavelength was not the wavelength of the reflection peak or even the center of gravity of the reflection curve which is almost symmetrical, but was a still shorter wavelength. The average wave numbers of the wavelengths used in this experiment were KRS-5—64 cm^{-1}, CsI—70 cm^{-1}, CsBr—85 cm^{-1}, KI—111 cm^{-1}, KBr—131 cm^{-1}, KCl—164 cm^{-1}, and NaCl—192 cm^{-1}. The uncertainty in these values is about ±2 cm^{-1}.
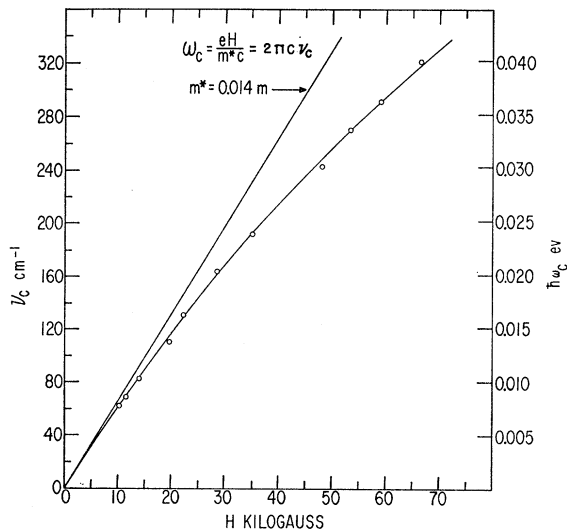

FIG. 2. Cyclotron resonance frequency as a function of magnetic field for n-type InSb at liquid nitrogen temperature.
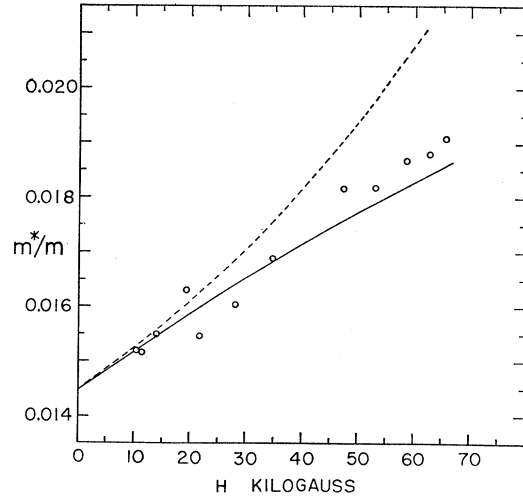

FIG. 3. Variations of effective mass with magnetic field in InSb. The dashed line is the theoretical result from fourth order effective-mass theory and the solid line is the theoretical result from the simplified Yafet theory. The experimental points are the circles.

3. EXPERIMENTAL RESULTS

Some experimental results are shown in Fig. 2. Here, the frequency of the observed absorption maximum obtained at 80°K is plotted against magnetic field. For comparison, the curve for a fixed mass of $0.014m$ is shown as a straight line. It is apparent that the position of the cyclotron absorption maximum does not vary linearly with magnetic field. The curvature is indicative of an increasing effective mass in the conduction band. Figure 3 is a plot of the effective mass $(m^*)_{\text{exp}}$ obtained from the data of Fig. 2 from the equation

$$(m^*)_{\text{exp}} = eH/\omega c.$$

The effective mass so defined is an average mass whose theoretical interpretation in terms of the nonparabolic nature of the conduction band is discussed in Sec. 4. The effective mass ratio is seen to be about 0.0145 at the bottom of the conduction band at $H=0$ and increases roughly linearly with H. The uncertainty in this value is slightly less than ±0.001. Figure 4 shows some of the absorption curves measured. The curve obtained at 80°K is superimposed on the curve obtained at 300°K to emphasize the change in band shape. An idea of the signal-to-noise ratio can be had from these curves. Note that the wavelength was fixed and the magnetic field varied. The field was changed from zero to maximum to zero, and the two "mirror image" line positions were averaged. Figure 5 shows the absorption band obtained at a fixed high field while varying the wavelength. The absorption band at room temperature was quite broad, the relative transmission persisting at about 50% from the short wavelength edge to the longest wavelengths studied. The radiation used was unpolarized. At 80°K the absorption band sharpened considerably and a satellite line was resolved

at a slightly lower energy than the main absorption line. Also, there was a region of broad absorption at still lower energy. The separation of the main line and satellite varied roughly linearly with magnetic field, although the scatter was too large to establish the exact dependence on magnetic field. In Fig. 5 the main line and satellite line occur at 337 and 309 cm^{-1} (0.0418 and 0.0383 ev) at 69.2 kilogauss and 80°K, while they occur at 301 and 276 cm^{-1} (0.0373 and 0.0342 ev) at 62.4 kilogauss and 25°K. Use of circularly polarized light indicated that the absorption was due to electrons rather than holes.

As shown in Fig. 5 the low-energy tail of the absorption at room temperature is reduced considerably at lower temperatures. However, even at the lower temperatures some structure is resolved in this tail using a prism monochromator and high magnetic fields. At lower magnetic fields, the separation of the satellite and main line is smaller. Consequently, when measurements were made at lower frequency with these lower fields using a KCl reststrahlen monochromator with poorer resolution, the satellite line was only indicated by a tail in the absorption band and not resolved. As shown in Fig. 4 at still lower frequency and magnetic field using KI reststrahlen, this satellite structure could not be seen, and the absorption band appeared symmetrical.

At 25°K the bands sharpened somewhat with the satellite still evident. The broad, low-energy absorption was reduced slightly.

It is interesting to note that Boyle and Brailsford[6] observed two impurity transitions in the same infrared region where some of the present data were obtained. Their sample was pure enough so that there was appreciable freezeout of carriers into the two lowest impurity levels below the conduction band. According to their work and that of Wallis and Bowlden,[7] a strong and a weak impurity transition occur near each other, forming a strong line and a weaker line to lower energy. The weak, lower energy impurity transition should have about the same energy as the cyclotron resonance transition. Study of their data shows that the weak absorption observed by Boyle and Brailsford falls very
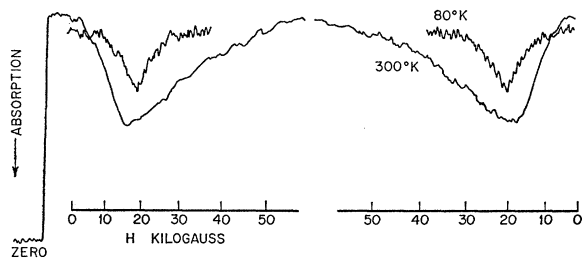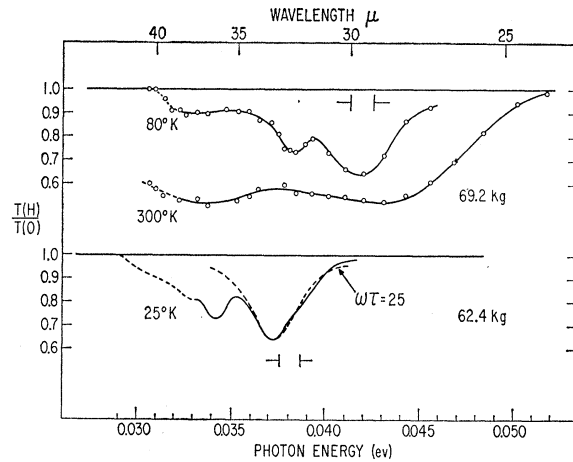

FIG. 5. Cyclotron resonance in n-type InSb at various temperatures and magnetic fields.

near the strong cyclotron line we observe. Considering the work of Sladek[8] and Keyes and Sladek,[9] it does not seem likely that there was appreciable freezeout in our experiments for the temperatures, magnetic fields and sample purities used.

The principal data presented here in Figs. 2 and 3 give a liquid nitrogen temperature effective-mass ratio of 0.0145 at the bottom of the conduction band. The original microwave cyclotron resonance data[1] at liquid helium temperature gave an effective-mass ratio of 0.013±0.001 near the bottom of the band. The impurity transition measurements of Boyle and Brailsford[6] at liquid helium temperature infer an effective-mass ratio of 0.0155 near the bottom of the conduction band. We believe that within experimental error, these low-temperature mass ratios agree with the liquid nitrogen temperature mass ratio reported here.

Figure 4 and Fig. 5 give a slight indication that the points of minimum transmission for the room temperature and liquid nitrogen temperature data do not coincide. Some of the other data not shown also suggest this. However, since the room temperature lines are broad, there is considerable uncertainty in locating the transmission minimum. This difference indicates that the room temperature effective-mass ratio is smaller than the mass ratio at 80°K by about 0.001 for all values of magnetic field measured.

By taking an average of the room temperature data, we estimate that the room temperature effective-mass ratio at the bottom of the band is about 0.0135 which is smaller than the liquid nitrogen temperature mass ratio by 0.001. Room-temperature cyclotron resonance data of Burstein, Picus, and Gebbie[2] give a mass ratio of 0.015 at 40 kilogauss. However, we believe that this value is low because of an error in magnetic field calibration and should be more nearly 0.016 which is in

FIG. 4. Cyclotron resonance in n-type InSb at 111 cm^{-1}.

[6] W. S. Boyle and A. D. Brailsford, Phys. Rev. 107, 903 (1957).
[7] R. F. Wallis and H. J. Bowlden, J. Phys. Chem. Solids 7, 78 (1958).
[8] R. J. Sladek, J. Phys. Chem. Solids 5, 157 (1958).
[9] R. W. Keyes and R. J. Sladek, J. Phys. Chem. Solids 1, 143 (1956).

better agreement with our room-temperature data near 40 kilogauss. The high-field, room-temperature cyclotron resonance measurements of Keyes et al.[3] have been discussed by Lax and Mavroides[5] who conclude that the room-temperature mass ratio is 0.010 at the bottom of the band. This result was obtained by using Kane's[10] formula for the effective-mass ratio

$$\frac{m}{m^*} \simeq \frac{2}{3}P^2\left(\frac{2}{E_G}+\frac{1}{E_G+\Delta}\right),$$

where P is a momentum matrix element between valence and conduction bands at $k=0$, E_G is a corresponding energy gap and Δ is the spin-orbit splitting in the valence band. Lax and Mavroides assumed that P and Δ are constants independent of temperature, that E_G is given by the experimental optical gap at the appropriate temperature, i.e., 0.24 ev at 4°K and 0.18 ev at 300°K, and that m^*/m has the value 0.013 at 4°K. If one uses the low-temperature mass ratio 0.0145 obtained in the present work, a similar calculation yields a room temperature mass ratio of 0.0115. We believe that the experimental errors in our room temperature measured value of 0.0135 are not sufficient to account for this discrepancy. A possible explanation of this discrepancy may be that P and Δ are not independent of temperature. Another possibility is that one should not use the full experimental change in optical gap in calculating E_G but rather only the dilational contribution to the change since Kane's formula is derived for a rigid lattice and contains no effects due to lattice vibrations. As pointed out by Moss[11] dilation accounts for one-third and lattice vibrations for two-thirds of the total change in gap between liquid nitrogen temperature and room temperature. If one uses only the dilational part of the change in band gap and uses the value 0.0145 for the low-temperature effective mass ratio, one obtains the value 0.0135 for the room-temperature mass ratio in agreement with our experimental result. It still remains to be shown, however, what modifications in Kane's formula for the effective-mass ratio will be produced by inclusion of lattice vibrational effects in the theory.

The frequency obtained from measuring the transmission of the sample may have to be corrected for possibly two reasons. As shown by Dresselhaus, Kip, and Kittel,[12] the position of the cyclotron absorption may be influenced by depolarization effects due to sample geometry. The observed position ω of the resonance does not yield the cyclotron frequency ω_c, but it is related to it by the relation

$$\omega_c=\omega[1-(\omega_L/\omega)^2],$$

where ω_L is a frequency given by

$$\omega_L=(LNe^2/m^*)^{\frac{1}{2}}.$$

In this equation L is a depolarization factor which depends on the sample geometry. As discussed by Dresselhaus, Kip, and Kittel,[13] this factor is small for a disk-shaped sample and the electric vector of the radiation in the plane of the sample. As the thickness of the sample increases, so that the disk becomes a thick cylinder, the factor L approaches $4\pi/\epsilon_0$, so that

$$\omega_L \rightarrow (4\pi Ne^2/m^*\epsilon_0)^{\frac{1}{2}}=\omega_P.$$

Here, ϵ_0 is the dielectric constant of the host lattice. This quantity ω_P is just the usual plasma frequency, the frequency at which a semiconductor becomes highly reflecting due to free carrier absorption. For the InSb sample used, the plasma frequency corresponds to a wavelength of about 500 microns. In view of the fact that the sample used in the present investigation was approximately $0.7\times0.5\times0.0015$ cm³, the value of ω_L is negligibly small compared to ω, so that $\omega_c=\omega$. Therefore, no correction to the observed frequency was made to obtain the cyclotron frequency.

There is another correction arising from the fact that in the present experiment, the transmission of the sample is measured and not the complex dielectric constant or real conductivity. For circularly polarized light, the real and complex dielectric constants of a material containing free electrons under the influence of a constant external magnetic field are

$$\epsilon_R=\epsilon_0-\frac{4\pi\sigma_0}{\omega}\frac{(\omega\pm\omega_c)\tau}{[1+(\omega\pm\omega_c)^2\tau^2]},$$

$$\epsilon_I=\frac{4\pi\sigma_0}{\omega}\frac{1}{[1+(\omega\pm\omega_c)^2\tau^2]},$$

where the dc conductivity $\sigma_0=Ne^2\tau/m^*$, ϵ_0 is the dielectric constant of the lattice, and the $\pm$ signs refer to right and left circularly polarized light. From these equations, one can compute the index of refraction, extinction coefficient, reflectivity, and transmission of the sample. The above equations illustrate some interesting magneto-optic effects. For magnetic field $H=0$, these equations yield the usual result that the reflectivity has a minimum and then quickly approaches a maximum of unity in the region of the plasma frequency ω_P. For low magnetic fields such that $\omega_c<\omega_P$, this minimum moves to higher frequency by an amount equal to $\frac{1}{2}\omega_c$. For higher magnetic fields, this minimum moves to still higher frequency, always remaining at a frequency slightly higher than ω_c. These effects are discussed by Boyle, Brailsford, and Galt,[14] and Lax

[10] E. O. Kane, J. Phys. Chem. Solids 1, 249 (1956).
[11] T. S. Moss, Optical Properties of Semiconductors (Academic Press, Inc., New York, 1959).
[12] G. Dresselhaus, A. F. Kip, and C. Kittel, Phys. Rev. 100, 618 (1955).
[13] G. Dresselhaus, A. F. Kip, and C. Kittel, Phys. Rev. 98, 368 (1955).
[14] W. S. Boyle, A. D. Brailsford, and J. K. Galt, Phys. Rev. 109, 1396 (1958).

and Wright.[15] Also, the difference between the minimum and maximum of reflectivity decreases as H increases. As applied to the particular InSb sample used in the present experiments, the equations show that whereas the real conductivity or complex dielectric constant peak at ω_c and are nearly symmetrical, the extinction coefficient and the transmission do not peak at ω_c but at a slightly higher frequency. Thus, the observed frequency should be corrected downward to obtain the cyclotron frequency. For the InSb sample used, this correction varies from about 0.3% at 300 cm^{-1} to 1% at 70 cm^{-1}. This correction is so small that it has not been made for the data presented here. However, the correction becomes larger the smaller $\omega_c\tau$ is and can amount to several percent in some III-V semiconductor samples.

The lattice absorption and reststrahlen in InSb fall in the region between 50 and 60 microns. The peak reflectivity occurs at 53.8 microns while measurements of the sample transmission indicated the fundamental lattice vibration absorption at 55.1 microns. The sample is at best a few percent transmitting from 52 to 58 microns and increases to about 30% on both sides of this lattice absorption region. Since the band pass of the optics using NaCl reststrahlen and crystal quartz is centered at 52.0 microns, exclusive of sample, there is some uncertainty as to the average wavelength of the energy absorbed in cyclotron resonance. Therefore, the NaCl point in Fig. 2 at 35 kilogauss is questionable even though it falls on the smooth curve.

4. THEORETICAL INTERPRETATION

The magnetic field dependence of the effective mass and the structure of the cyclotron resonance absorption band observed at room temperature and at low temperature can be interpreted in terms of the nonparabolic character of the conduction band as established by Kane.[10] Wallis[16] has developed a theory of conduction-electron cyclotron resonance in InSb taking into account k^4 terms in the conduction-electron energy expansion, but neglecting spin effects. His treatment predicts that each Landau level becomes nonparabolic to a different degree and the separation between succeedingly higher Landau levels at $k=0$ decreases. Vertical transitions occur between the two lowest Landau levels for values of $k_z\neq0$. (We assume throughout this paper that the magnetic field is in the z direction.) Consequently, these transitions will produce a low-energy tail. Also, the transitions between higher Landau levels will occur at lower energy and will contribute to the tail and possibly lead to resolvable subsidiary peaks. At lower temperatures the number of electrons in higher Landau levels will decrease, and the number of electrons with large k_z values will also decrease. Therefore, the tail due to these two kinds of

transitions should be reduced at lower temperatures. A further consequence of the nonparabolic character of the conduction band is that the separation of the Landau levels is not simply proportional to the magnetic field, so that the effective mass determined from the cyclotron resonance frequency has an apparent magnetic field dependence.

The work of Roth et al.[17] on magneto-optic phenomena and of Bowers and Yafet[18] on magnetic susceptibility has shown that the spin-orbit interaction produces very important effects in InSb. We have therefore extended the work of Wallis to include the spin-orbit interaction and the interaction of the spin with the external magnetic field. To fourth order in effective mass theory[16] and taking into account only the interactions of the conduction, light-hole, heavy-hole, and split-off bands, the energies for the Landau levels of the conduction band can be written as

$$E(l, k_z, \pm)$$
$$= \mathcal{E}_c + J_c + \hbar\omega_c(l+\tfrac{1}{2}) + \hbar^2 k_z^2/2m^* \pm \tfrac{1}{4}(m^*/m)\hbar\omega_c g_0^*$$
$$\pm K_0(\hbar\omega_c/E_G)\hbar\omega_c(l+\tfrac{1}{2}) \pm K_1(\hbar\omega_c/E_G)\hbar^2 k_z^2/2m^*$$
$$+ (K_2/E_G)[\hbar\omega_c(l+\tfrac{1}{2})+\hbar^2 k_z^2/2m^*]^2, \quad (1)$$

where

$$\omega_c = eH/m^*c, \quad (1a)$$

$$J_c = -\tfrac{1}{2}(\hbar\omega_c/E_G)[(1-y)/(2+x)^2]$$
$$\times\{[\tfrac{1}{3}(1-x)^2 - (2+x^2)](2+x)y$$
$$+\tfrac{1}{2}(1-x^2)(1+x)(1-y)\}, \quad (1b)$$

$$g_0^* = 2\{1 - [(1-x)/(2+x)][(1-y)/y],\} \quad (1c)$$

$$K_0 = (1-y)(1-x)\{[(2+\tfrac{3}{2}x+x^2)$$
$$\times(1-y)/(2+x)^2] - \tfrac{2}{3}y\}, \quad (1d)$$

$$K_1 = (1-y)[(1-x)/(2+x)]$$
$$\times\{[(2+\tfrac{3}{2}x+x^2)(1-y)/(2+x]$$
$$-\tfrac{2}{3}(1-x)y\}, \quad (1e)$$

$$K_2 = -[(1+\tfrac{1}{2}x^2)/(1+\tfrac{1}{2}x)](1-y)^2, \quad (1f)$$

$$x = [1+(\Delta/E_G)]^{-1}, \quad (1g)$$

$$y = m^*/m. \quad (1h)$$

In the above equations l is the Landau quantum number and k_z is the propagation constant parallel to the magnetic field. The quantities $\mathcal{E}_c$, E_G, Δ, and m^* specify at $k=0$ the energy of the conduction bands, the separation of the valence and conduction bands, the spin-orbit splitting of the valence bands, and the curvature effective mass of the conduction band, respectively, in the absence of a magnetic field. The constant g_0^* is the effective g factor[17] for small magnetic fields at $k_z=0$, while K_0 and K_1 specify the change in g factor with Landau quantum number l and with k_z, respectively. For zero magnetic field the conduction

[15] B. Lax and G. B. Wright, Phys. Rev. Letters 4, 16 (1960).
[16] R. F. Wallis, J. Phys. Chem. Solids 4, 101 (1958).

[17] L. M. Roth, B. Lax, and S. Zwerdling, Phys. Rev. 114, 90 (1959).
[18] R. Bowers and Y. Yafet, Phys. Rev. 115, 1165 (1959).

band energy is given by

$$E(k) = \mathscr{E}_c + \hbar^2 k^2 / 2m^* + K_2 \hbar^4 k^4 / 4m^{*2} E_G, \qquad (2)$$

so that K_2 is the fourth order constant and corresponds, aside from a constant factor, to $\mathscr{E}_c{}^{xxxx}$ in the earlier treatment of Wallis. It may be noted that the value of K_2 is quite insensitive to the value of Δ so that the expression previously given[16] for $\mathscr{E}_c{}^{xxxx}$ remains quite accurate even for $\Delta \gg E_G$.

Since the value of g_0^* is approximately -50 for InSb, the lowest Landau level in the conduction band has energy $E(0, k_z, +)$. The principal peak in the cyclotron resonance absorption spectrum at liquid nitrogen temperatures and below then corresponds to vertical transitions from the $E(0, k_z, +)$ level to the $E(1, k_z, +)$ level. In InSb the most important transitions involve $k_z = 0$ for carrier concentrations $\sim 10^{15}$ cm^{-3}, magnetic fields > 10 kilogauss, and liquid nitrogen temperatures. The effective mass $(m^*)_{\mathrm{exp}} = (eH/\omega_c)$ calculated from the experimental value for the frequency of maximum cyclotron absorption should therefore correspond rather closely to transitions between the energy levels $E(0, 0, +)$ and $E(1, 0, +)$ when the low-temperature data is used. A magnetic field-dependent effective mass can accordingly be defined by

$$\frac{1}{m^*(H)} = (c/\hbar eH)[E(1, 0, +) - E(0, 0, +)] \qquad (3a)$$

$$= \frac{1}{m^*}[1 + (K_0 + 2K_2)(\hbar\omega_c/E_G)]. \qquad (3b)$$

Values of $m^*(H)$ have been calculated from Eq. (3b) using the values $m^* = 0.0145m$, $E_G = 0.225$ ev, and $\Delta = 0.9$ ev. The results are indicated by the dotted curve in Fig. 3. The slope of the dotted curve agrees rather well with the experimental data at low magnetic fields, but is significantly too high at the higher fields.

A considerable improvement in the theoretical values can be obtained by calculating the energies of the Landau levels using the method of Bowers and Yafet.[18] In this method the interactions of the conduction, valence and split-off bands are treated exactly, while other bands are neglected to first approximation. By neglecting certain terms of orders m^*/m and E_G/Δ,
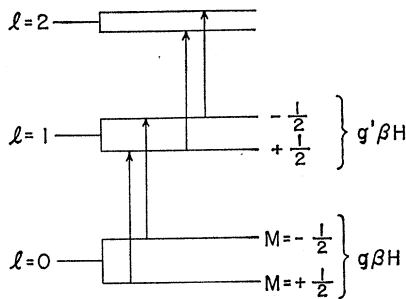

Fig. 6. Spin splitting of Landau levels for conduction band in InSb.

one can obtain the following rather simple expression[5] for the energies of the conduction band Landau levels:

$$E(l, 0, \pm) = \tfrac{1}{2}E_G\{1 + [1 + 2(2l + 1 \mp \tfrac{1}{2})(\hbar\omega_c/E_G)]^{\frac{1}{2}}\}. \qquad (4)$$

Equation (4) is the magnetic field analog of Eq. (13) in Kane's theory of the band structure of InSb. The values of $m^*(H)$ calculated from Eqs. (3a) and (4) for InSb are given by the solid line in Fig. 3. This theoretical result agrees with the experimental points to within experimental error. In principle, one can improve the theory by retaining terms of all orders in m^*/m and E_G/Δ and also including interactions of higher bands.

We have made such a calculation of the energies $E(0, 0, +)$ and $E(1, 0, +)$ for magnetic fields up to 100 kilogauss using the method of Bowers and Yafet. The free mass terms and the free spin terms are in-
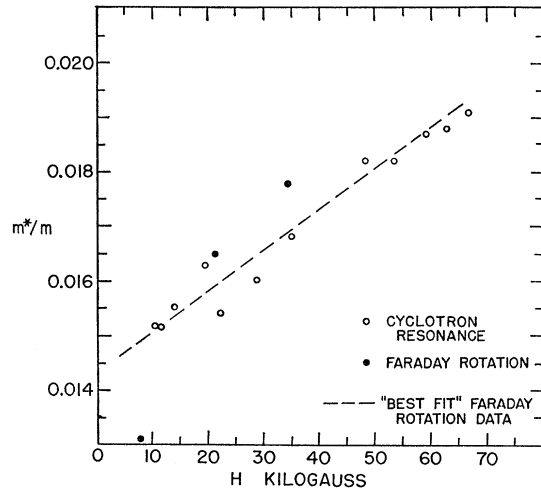

Fig. 7. Comparison of effective masses from Faraday rotation and cyclotron resonance experiments at liquid nitrogen temperature.

cluded to first order. First-order contributions involving Kane's higher band interaction constants B and C are also included. The values for B and C were taken to be $-(5/3)$ and $-(8/3)$ atomic units, respectively, as given by Bowers and Yafet. The results for the effective mass ratio computed from Eq. (3a) differ insignificantly from the solid line in Fig. 3 up to 70 kilogauss.

Denoting the Landau levels by the notation $(l, \pm)$, it is of interest to calculate the energy differences associated with the transitions $(0, +) \to (1, +)$, $(0, -) \to (1, -)$, and $(1, +) \to (2, +)$. The results obtained using Eq. (4) at 69.2 kilogauss are 0.0430 ev, 0.0378 ev, and 0.0341 ev, respectively. Comparison of these values with the 80°K data in Fig. 5 indicates that the principal peak at 0.042 ev is due to the $(0, +) \to (1, +)$ transition, the subsidiary peak at 0.038 ev is due to the $(0, -) \to (1, -)$ transition while the long-wavelength tail is at least partially due to the $(1, +) \to (2, +)$

transition. It may be noted that the lack of coincidence of the transitions $(0, +) \rightarrow (1, +)$ and $(0, -) \rightarrow (1, -)$ is due to the change in the effective g factor with energy into the conduction band.[18] These transitions are illustrated in Fig. 6 in which the g factor is shown to decrease as l increases.

The relationship between effective masses determined by cyclotron resonance and those determined by Faraday rotation can be elucidated using the fourth order Eqs. (2) and (3b). According to Stephen and Lidiard,[19] the effective mass measured by Faraday rotation on degenerate samples in small magnetic fields is given by

$$\frac{1}{m^*(E)} = (1/\hbar^2 k)\frac{dE(k)}{dk}, \qquad (5)$$

evaluated at the Fermi surface. By using Eq. (2) one obtains

$$\frac{1}{m^*(E)} = \frac{1}{m^*}\{1+2(K_2/E_G)(\hbar^2 k^2/2m^*)\}_F \qquad (6a)$$

$$\simeq \frac{1}{m^*}\{1+2(K_2/E_G)[E(k)-\mathcal{E}_c]\}_F \qquad (6b)$$

$$= \frac{1}{m^*}\{1+(K_0+2K_2)[2K_2/(K_0+2K_2)]$$
$$\times[E(k)-\mathcal{E}_c]/E_G\}_F. \qquad (6c)$$

Comparison of Eqs. (6c) and (3b) indicates that m^* (H) and $m^*(E)$ will be the same if

$$[E(k)-\mathcal{E}_c]_F = [1+\tfrac{1}{2}(K_0/K_2)]\hbar\omega_c. \qquad (7)$$

For InSb, the ratio $K_0/K_2 = -0.41$. Using Eq. (7) we have calculated equivalent magnetic fields for the Faraday rotation data obtained by Smith et al.[20] on InSb samples doped to varying degrees with donor impurities. The results for the effective masses in the purer samples are specified by solid circles in Fig. 7. The open circles are the cyclotron resonance effective masses reported in the present paper. Considering the scatter of the Faraday data the agreement is reasonably good. The dashed line in Fig. 7 specifies effective masses derived from a curve which "best fits" the Faraday data of Smith et al.

We wish to emphasize the difference in experimental conditions for the cyclotron resonance experiments reported here and the Faraday rotation experiments of Smith et al. The cyclotron resonance work was done at high magnetic fields with rather pure samples, $\hbar\omega_c$ $\gg[E(k)-\mathcal{E}_c]_F$. The Faraday work was done at low magnetic fields with impure samples, $\hbar\omega_c \ll [E(k)-\mathcal{E}_c]_F$.

[19] M. J. Stephen and A. B. Lidiard, J. Phys. Chem. Solids 9, 43 (1959).
[20] S. D. Smith, T. S. Moss, and K. W. Taylor, J. Phys. Chem. Solids 11, 131 (1959).
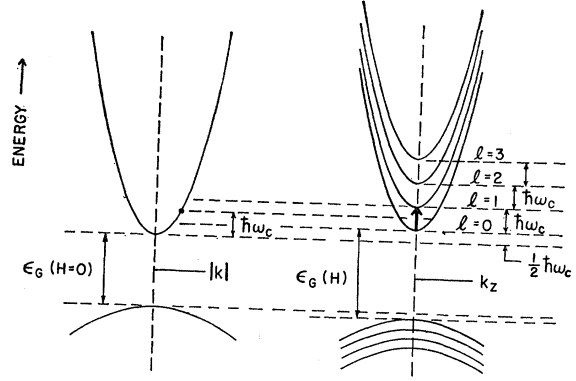

FIG. 8. Simple energy bands of a semiconductor in the absence and presence of a magnetic field.

Both procedures provide a means of probing the non-parabolic character of the conduction band and the results may be correlated using Eq. (7).

A simple physical picture of the relationship between effective masses determined by cyclotron resonance and Faraday rotation can be given if one neglects the small term involving K_0 in Eqs. (3b) and (7). The Faraday rotation effective mass is $(1/\hbar^2 k)(dE/dk)$ evaluated at the Fermi surface. Ordinarily the magnetic field is small, so that to first approximation the Fermi surface is not shifted by the magnetic field. The situation is indicated schematically in Fig. 8. The cyclotron resonance effective mass is derived primarily from a transition of the electron from the $l=0$ Landau level at an energy $\sim\tfrac{1}{2}\hbar\omega_c$ above the bottom of the conduction band to a level at an energy $\sim\tfrac{3}{2}\hbar\omega_c$. The mean energy of the electron during the transition is then roughly $\hbar\omega_c$ above the band edge. This situation is illustrated in Fig. 8. Consequently, one may expect the Faraday and cyclotron resonance effective masses to be roughly the same when $\hbar\omega_c$ in cyclotron resonance is equal to $[E(k)-\mathcal{E}_c]_F$ in the low-field Faraday effect. Inclusion of the interaction of the electron spin with the magnetic field complicates the above argument if the effective g factor is large as in InSb. A better comparison can then be obtained using Eq. (7).

A possible source of discrepancy between Faraday and cyclotron resonance effective masses is the modification of the energy bands by the impurities used to adjust the Fermi level in the Faraday experiments. This effect seems to be small in InSb for impurity concentrations less than 10^{18} cm^{-3}.

ACKNOWLEDGMENTS